Structure–property relations of polyethertriamine-cured bisphenol-A-diglycidyl ether epoxies*

Roger J. Morgan, Fung-Ming Kong and Connie M. Walkup
Lawrence Livermore National Laboratory, Livermore, CA 94550, USA
(Received 16 September 1982; revised 25 April 1983)

The relations between the chemical and physical network structure, the deformation and failure processes and the tensile mechanical properties of polyethertriamine-cured bisphenol-A-diglycidyl ether epoxies are reported for a series of epoxy glasses prepared from a range of polyethertriamine concentrations. Near-infra-red spectroscopy indicates that these glasses form exclusively from epoxide–amine addition reactions. Their T_g exhibits a maximum and swell ratio a minimum at the highest crosslink density. Stress-birefringence studies reveal that these highly crosslinked glasses are ductile and undergo necking and plastic deformation. The plastic deformation initially occurs homogeneously but ultimately becomes inhomogeneous and shear bands develop. Tensile failure occurs in the high strain shear band region. The ultimate tensile strain of these epoxies attains a maximum of 15% for the highest crosslinked glass. Off stoichiometric networks fail at lower strains because such networks inherently contain more defects in the form of unreacted ends. The density, yield stress, tensile strength, and modulus of these glasses all decrease with increasing polyethertriamine concentration as a result of increasing free volume because of the poor packing ability of the amine molecule. A slight minimum is superimposed on this downtrend in density and modulus with increasing amine content at the highest crosslink density because of geometric constraints imposed on segmental packing by the network crosslinks. The ability of these crosslinked glasses to undergo deformation is discussed in terms of the free volume and the crosslinked network topography. Network failure is considered in terms of stress-induced chain scission which is determined by the concentration ad extensibility of the least extensible network segments.

Keywords Epoxies; cure reactions; network structure; mechanical properties; deformation process; failure process

INTRODUCTION

The increasing use of high-performance, fibrous composites in critical structural applications has led to a need to predict the lifetimes of these materials in service environments. To predict the durability of a composite in service environment requires a basic understanding of (1) the microscopic deformation and failure processes of the composite; (2) the significance of the fibre, epoxy matrix and fibre-matrix interfacial region in composite performance; and (3) the relations between the structure, deformation and failure processes and mechanical response of the fibre, epoxy matrix and their interface and how such relations are modified by environmental factors.

This paper considers the structure–property relations of epoxy matrices, with specific emphasis on amine-cured epoxides. In attempts to correlate the structure–property relations of amine-cured epoxides, there have been a number of studies on the mechanical properties of these glasses as a function of epoxide: amine ratios and the chemical structure of the constituent epoxide and amine monomers[1-15]. Generally, there is no direct correlation between the chemistry of the epoxide and amine monomers and the mechanical properties of epoxies with the exception that as the distance between crosslinks becomes shorter, these glasses become more brittle[1,10,15]. Also, for a specific amine-cured epoxide system, the T_g is always highest for the fully reacted, highest crosslink density glass[3,6,9,12,16-18].

There are a number of reasons why there is not a simple correlation between the chemistry of the starting materials and the mechanical properties of the resultant cured epoxy glass. Firstly, the chemistry of the epoxy network may not always be simple. Amine-cured epoxy networks are generally assumed to result exclusively from addition reactions of epoxide groups with primary and secondary amines[16]. However, these reactions are often incomplete due to steric and diffusional restrictions and additional reactions such as epoxide homopolymerization can occur[8,12,13,16,19-28]. The physical structures of epoxies are also complex on a macroscopic and microscopic scale and have not been characterized in detail. Macroscopically, the crosslinked networks are inhomogeneous because of voids and possible distributions in the crosslink density. On a more microscopic level, details of the local free volume, the rotational isomeric configurations of segments between crosslinks, chain end defects, and any bond angle and length distortions produced to form the crosslinked networks are generally unknown. These chemical and physical structural parameters are significant in the

* This work was carried out under the auspices of the US Department of Energy by Lawrence Livermore National Laboratory under Contract No. W-7405-Eng-48

0032-3861/84/030375-12$03.00

deformation and failure processes and mechanical response of the glassy crosslinked networks. However, few studies have been carried out on the microscopic deformation and failure processes of epoxy glasses[13,27,29,30]. Therefore, at present there are considerable gaps in the understanding of the structure–property relations of epoxies.

To further the understanding of crosslinked epoxies, this paper reports structure–property studies of a series of polyethertriamine-cured bisphenol-A-diglycidyl ether (DGEBA) epoxies, the chemical structures of which are well characterized. Different epoxy networks were produced by varying the epoxide:amine ratios. The physical structure, deformation and failure processes and mechanical properties of these glasses are reported and are correlated with the systematic chemical structural changes in this epoxy series. The high ductilities of these epoxies and their relative insensitivity to inherent fabrication flaws were advantageous in correlating their network structure with their mechanical response.

EXPERIMENTAL

Materials

Pure DGEBA, DER 332 (Dow*) epoxide monomer was used in this study and was cured with an aliphatic polyethertriamine, Jeffamine T403 (Jefferson). The chemical structures of the amine and epoxide monomers are shown in *Figure 1*. The epoxide and amine equivalent weights determined by chemical titration were 175.15 and 82.92 g, respectively. If these systems form exclusively from epoxide–amine addition reactions, ≈47 amine parts per hundred epoxide parts (phr) T403 are required for complete cure. A range of epoxies with 25–75 phr T403 was prepared. The DGEBA epoxide monomer was preheated to 60°C to melt any crystals present[8] prior to mixing with the T403. After mixing the two monomers, the mixtures were vacuum degassed and cast between glass plates separated by 0.3 cm thick Teflon spacers. A thin layer of release agent (DC-20 Dow) was baked onto each plate prior to casting. The epoxy sheets were cured

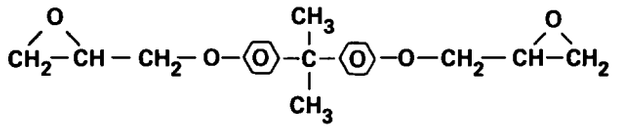

Diglycidyl ether of bisphenol A
(DOW DER 332)

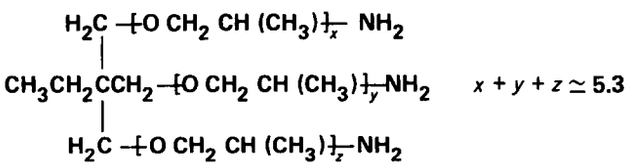

$x + y + z \simeq 5.3$

Polyether triamine
(Jefferson T403)

Figure 1 Chemical structure of DGEBA epoxide and T403 polyethertriamine curing agent

between the glass plates at room temperature for 24 h, post-cured at 85°C for 16 h, and then slowly cooled at ≈2°C min^{-1} to room temperature. All specimens used for physical structural characterization and mechanical property tests were fabricated from these epoxy sheets.

Methods

Near-infra-red spectroscopy (Cary) 14 spectrophotometer) was used to study the cure reactions and the resultant chemical structure of the epoxies. A correct portion of epoxide and amine were mixed, degassed, and poured into a glass cell. To reduce the path length, a thin glass plate was inserted. A copper constantan thermocouple was used to control the test temperature. Each epoxy mixture was scanned at room temperature for 24 h and at 85°C for 16 h. The absorbances of the epoxide (A_e) and phenyl (A_p) groups were monitored at 2.205 and 2.160 μm, respectively. As the phenyl group does not participate in any of the chemical reactions, the absorbance of this group was utilized as an internal standard. The epoxide group consumption was determined by monitoring the changes in the $A_e:A_p$ ratio with cure time.

A differential scanning calorimeter (d.s.c.) (Du Pont 910) was used to monitor the T_g's of the epoxies. The heating rate was 10°C min^{-1}. The dynamic mechanical properties of the epoxies were monitored by a Rheometric mechanical spectrometer (Model RMS-7200). Epoxy specimens with dimensions of 6.4 × 1.3 × 0.3 cm were torqued at an oscillating frequency of 1.0 Hz. The shear storage (G') and loss (G'') moduli and tan δ were determined from −160° to +140°C. The densities of the epoxies were determined in density gradient columns. Swelling studies were carried out on 1 × 1 × 0.3 cm epoxy specimens that were immersed in methylethylketone for seven days. The weights (w) and volumes (v) of the specimens were measured prior to (w_i and v_i) and after (w_f and v_f) immersion and the swelling ratio v_f/v_i determined.

For the mechanical tensile tests, dogbone-shaped specimens with a gauge length of 7.5 cm and a width of 1.3 cm were cut from the cast epoxy sheets. After polishing the specimen edges along the gauge length, the specimens were annealed at 85°C under vacuum for 1.5 h to remove any sorbed moisture and release any fabrication strains. The specimens were stored in a desiccator prior to testing. All tensile tests were carried out at room teperature on a mechanical tester (Instron, TTDM) at a crosshead speed of 0.5 cm min^{-1}. The fracture topographies of the failed specimens were documented by optical microscopy (Zeiss).

The deformation modes were monitored with a polariscope (Photoelastic Inc.) as a function of stress for epoxies with 37, 47 and 57 phr T403). An attached camera was used to record the birefringence patterns.

RESULTS AND DISCUSSION

Chemical structure

Amine-cured epoxy networks generally form exclusively from epoxide-amine addition reactions, i.e.:

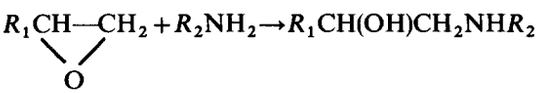

* Reference to a company or product name does not imply approval or recommendation of the product by the University of California or the US Department of Energy to the exclusion of others that may be suitable

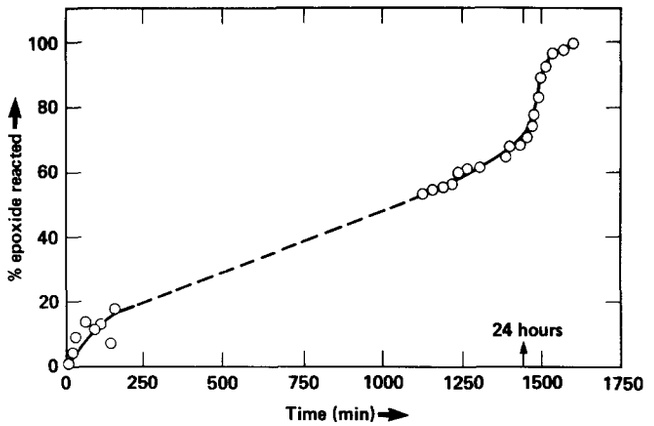

Figure 2 Epoxide consumption during cure at 23°C for 24 h followed by postcure at 85°C for DGEBA–T403 (47 phr T403) epoxy

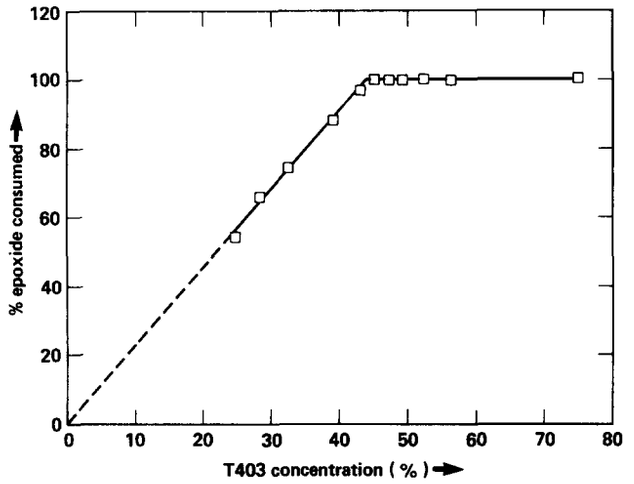

Figure 3 Ultimate percent epoxide consumption *versus* T403 concentration for 24 h cure at 23°C followed by 85°C postcure for DGEBA–T403

For all the amine hydrogens to react with epoxide groups in the DGEBA–T403 system exclusively by epoxide–amine additon reactions would require a stoichiometric quantity of 47 phr T403 based on the chemically-determined equivalent weights of the DGEBA and T403 reactants.

The epoxide consumption during cure was monitored by near-i.r. as a function of T403 concentration (25–75 phr) for a 24 h cure at 23°C followed by a postcure at 85°C. In *Figure 2* a plot of epoxide consumption during cure is illustrated for the DGEBA–T403 (47 phr T403) epoxy. (A period of 10 min was used to heat the epoxy from 23° to 85°C). For this epoxy, all the epoxide groups are consumed after about 200 min at 85°C. Similar plots were made for all epoxy systems in the 25–75 phr T403 concentration range. The i.r. measurements were truncated when either a 100% epoxide consumption occurred or the epoxide consumption ceased to change with time at 85°C. The ultimate percentage epoxide consumptions at 85°C are plotted as a function of T403 concentration in *Figure 3*. All epoxide groups are consumed at $\geqslant$45 phr T403. The lowest T403 concentration of 45 phr for full epoxide consumption is slightly power than the 47 phr T403 predicted from chemical analysis of the starting materials and assuming exclusively epoxide–amine addition reactions. This slight discrepancy could be due to insufficient accuracies in (1) the chemical titration procedures to determine the DGEBA and T403 equivalent weights and/or (2) in the near-i.r. to detect small differences in epoxide concentrations. In the 25–45 phr T403 range in *Figure 3*, the epoxide consumption levels fall on a straight line which, when extrapolated, goes through the origin. This data indicates that the DGEBA–T403 epoxies form exclusively from epoxide–amine addition reactions which proceed to completion without any additional epoxide consumption occurring as a result of side reactions.

The epoxide consumptions were also monitored for an 85°C cure alone. For the DGEBA–T403 (47 phr T403) epoxy, the cure reaction is complete after about 300 min as shown in *Figure 4*. A plot of epoxide consumption *versus* T403 concentration for a 16 h cure at 85°C is illustrated in *Figure 5*. This plot exhibits similar features as that plot for the 24 h, 23°C + 85°C postcured epoxies. Hence, the near-i.r. studies indicate that the DGEBA–T403 epoxies form exclusively from epoxide–amine addition reactions when cured either at 23°C, 24 h + 85°C postcure or at 85°C.

Network structure

The physical network structures and the average

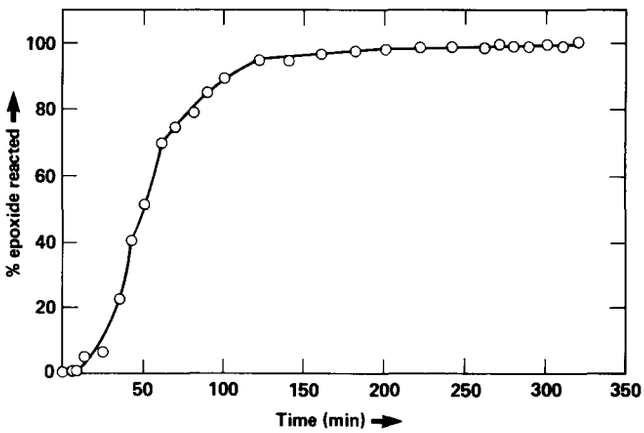

Figure 4 Epoxide consumption *versus* cure time at 85°C for DGEBA–T403 (47 phr T403) epoxy

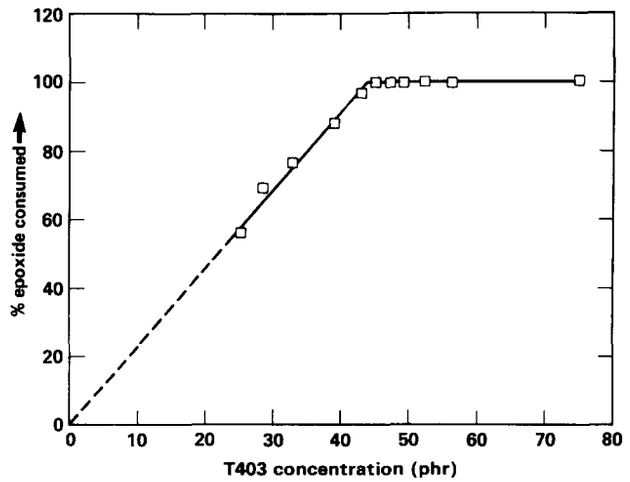

Figure 5 Ultimate percent epoxide consumption *versus* T403 concentration for 85°C cure of DGEBA–T403 epoxies

Table 1 Network structures and M_c for DGEBA–T403 epoxies

T403 concentration (%)	Structure	Comments	M_c
23.7	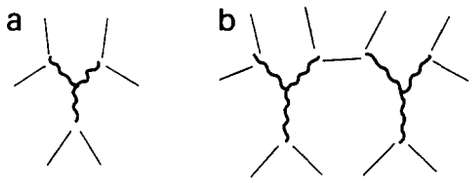	All $-NH_2$ and $-NH$ groups react;  (a) one — C(O)C — group reacts on each DGEBA molecule; (b) In some DGEBA molecules both — C(O)C — groups react whereas in others no — C(O)C — groups react	∞
47.3	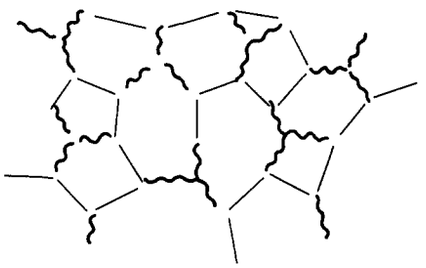	All $-NH_2$, $-NH$ and 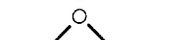 — C(O)C — groups reacted completely. A network of interconnected rings	258
94.7	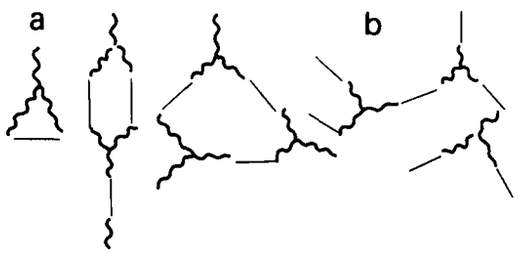	All $-NH_2$ and  — C(O)C — groups react; no $-NH$ groups react. (a) Ring and (b) branched structures	682
142.0	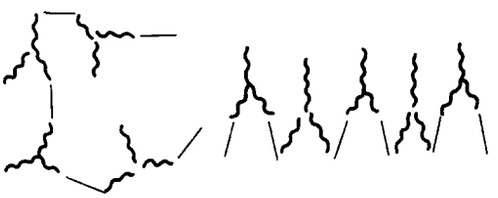	All 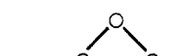 — C(O)C — groups react; 2/3 NH_2 groups react; no NH groups react; (a) branched and (b) linear structures	∞
	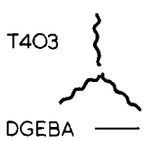		

molecular weight between crosslinks, M_c, for DGEBA–T403 epoxies as a function of T403 concentration were determined and are illustrated in *Table 1*. These network structures and M_c values were ascertained based on the chemical and physical structure of the DGEBA and T403 monomers and the following assumptions: (1) the cure reactions and network formation result exclusively from epoxide–amine addition reactions; (2) all primary amine hydrogens react with epoxide groups prior to the onset of secondary amine–epoxide addition reactions. The latter assumption is an approximation that simplifies the molecular description of the network structure. In fact, both the primary and secondary amine–epoxide reactions occur simultaneously, but the faster primary amine–epoxide reaction predominates in the early stages of cure and the slower secondary amine–epoxide reaction predominates in the later stages of cure. The presence of bulky groups in the vicinity of the amine group are known to preferentially slow the reaction rate of the secondary amine hydrogen relative to the primary amine hydrogen.[31–33] Molecular models indicate that the $-CH_3$ group adjacent to the NH_2 group in the T403 molecule would produce sufficient steric interference to significantly and preferentially slow the rate of secondary amine–epoxide reactions.

The functionalities and flexibilities of the DGEBA and T403 structures allow a variety of ring structures to form in the fully crosslinked DGEBA–T403 (≈47 phr T403) epoxy network. These chemically different series of rings can occur in the epoxy network and are illustrated in

Table 2. In addition, hybrids of these basic ring structures can also occur. Molecular models of these ring structures indicate all such structures illustrated in *Table 2* are sterically possible, primarily due to the flexibility of the DGEBA and T403 segments that make up the sides of the rings. Molecular models of the rings indicate that their sides can pack relatively well, with the exception of the three-sided rings, when such rings are considered in isolation from their neighbours. However, when the packing and steric requirements of interconnected neighbouring rings are considered, it is evident that the ability of the sides of the rings to pack efficiently is severely restricted and will be inhibited the most for the highest crosslink density network.

The M_c values illustrated in *Table 1* are plotted *versus* T403 concentration in *Figure 6* as the continuous line. The circular data points in this plot are determined from dynamic mechanical measurements and are discussed later. A more rapid increase in M_c with T403 concentration occurs on the excess epoxide side of stoichiometry relative to the excess T403 side.

Physical properties

The physical properties of the DGEBA–T403 epoxies as a function of T403 concentration can be understood in terms of the network structures discussed previously.

In *Figure 7*, the T_g's of the DGEBA–T403 epoxies, determined from d.s.c. measurements, are plotted *versus*

Table 2 Ring structures in DGEBA–T403 epoxy networks

Series (A) Sides of rings consist of (1 DGEBA segment + 2 arms of the T403 molecule) n

Where n = 1, 2, 3, . . .

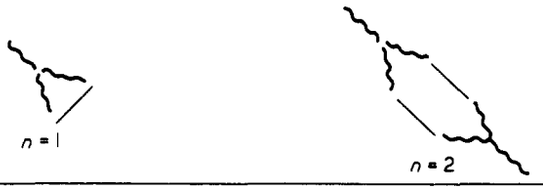

Series (B) Sides of rings consist of (2 DGEBA segments + 2 arms of T403 molecule) n

Where n = 1, 2, 3, . . .

Series (C) Sides of rings consist of (2 DGEBA segments + n DGEBA segments)

Where n = 1, 2, 3, . . .

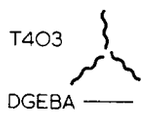

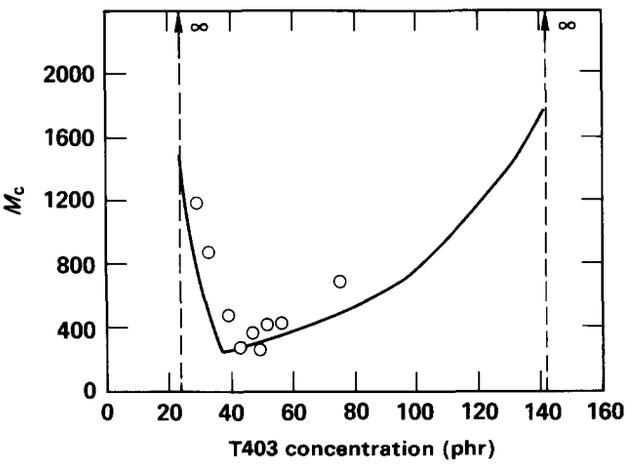

Figure 6 M_c *versus* T403 concentration for DGEBA–T403 epoxies; continuous line determined from chemistry of cure reactions; circular data points determined from G' values above T_g

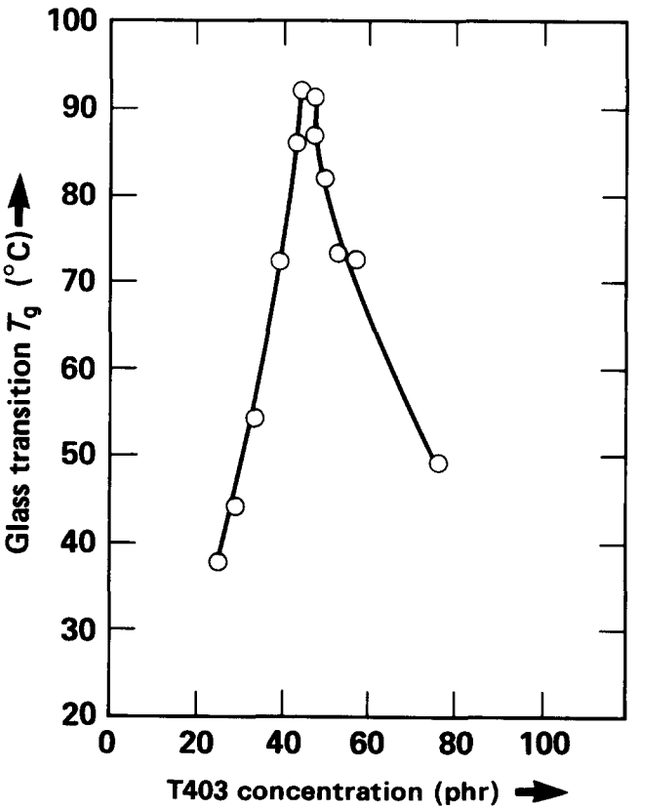

Figure 7 T_g *versus* T403 concentration for DGEBA–T403 epoxies

T403 concentration. The highest T_g, 93°C, is exhibited by the epoxy with the highest crosslink density at ≈45 phr T403, which is consistent with studies on other epoxy systems[3,6,9,12,16–18]. The T_g decreases less sharply with T403 concentration on the excess T403 side of stoichiometry because M_c increases less sharply on this side of stoichiometry.

In *Figure 8*, the swelling ratios of the epoxies are plotted as a function of T403 concentration. This ratio exhibits a minimum at stoichiometry and also increases less sharply with T403 concentration on the excess T403 side of stoichiometry. This data is consistent with the relation between crosslink density and T403 concentration. The

soluble fraction of 0.4 wt% in the DGEBA–T403 (47 phr T403) epoxy in the swelling agent was negligible.

A plot of the 23°C density of the DGEBA–T403 epoxies *versus* T403 concentration, in *Figure 9*, reveals the density progressively decreases with increasing T403 concentration. A slight inflection or minimum is superimposed on this downtrend at the T403 stoichiometric ratio, even when the outer data points of the scatter are considered. The inability of the three-armed T403 molecule to pack as well as the more linear DGEBA molecule causes a progressive density decrease with increasing T403 concentration. The apparent minimum in the density that is superimposed on this downtrend at the highest crosslink density is caused by the geometric constraints imposed on segmental packing by the crosslinked network geometry. Molecular models indicate that as the crosslink density of the network increases, the packing efficiency decreases. From compressibility studies, Findley and Reed[34] report lower crosslinked epoxies are more compact. Also, diffusion studies of H_2O and O_2 in crosslinked glasses indicate that the permeabilities will exhibit maxima at the highest crosslink density if the units that form the network inhibit close packing because of steric restrictions[35–37]. (The diffusion of He in thin DGEBA–T403 epoxy films as a function of T403 concentration was studied, but because of the sensitivity of the measurements to fabrication defects in the films, the data was inconclusive.)

The dynamic mechanical properties of the DGEBA–T403 epoxies were monitored as a function of T403 concentration in the −150°–140°C range. Plots of the logarithm of the shear storage (G') and loss (G'') moduli and $\tan\delta$ *versus* temperature are shown in *Figure 10* for DGEBA–T403 (47 phr T403) epoxy. A secondary glass transition, T_{gg}, (≈ -60°C) and a primary T_g ($\approx$90°C) are evident as maxima in $\log G''$ and $\tan\delta$ at these temperatures. A plot of T_g *versus* T403 concentration determined from the dynamic mechanical data exhibited similar characteristics as that plot determined from d.s.c. measurements in *Figure 7*. The secondary glass transition, T_{gg}, of the DGEBA–T403 epoxies exhibits a maximum temperature, ≈ -60°C, for the stoichiometric epoxy containing about 45 phr T403. The T_{gg} follows the same trend as the primary T_g with T403 concentration. The intensity of the T_{gg} in the -150°–(T_g 50°C) range also exhibits a maximum for the epoxy with the highest crosslink density. This observation implies the network segments responsible for the glassy state molecular motion associated with T_{gg} possess the greatest mobility at the highest crosslink density. The ability of polymeric segments to undergo molecular motion in the glassy state depend on both inter- and intramolecular interactions[38–40]. In this case, the molecular motion is enhanced for the higher crosslinked glasses because these glasses have greater free volume as a result of the packing constraints imposed by the crosslinks.

The storage modulus, G', at 23°C exhibits a minimum for the highest crosslink density epoxy which further supports the contention that the crosslinks inhibit intermolecular packing and enhance network flexibility.

The dynamic mechanical data was used to determine the molecular weight between crosslinks, M_c, for the DGEBA–T403 epoxies. The values of log G' above T_g were determined in the 100°–120°C region where the shear modulus is independent of temperature. At higher temperatures, > 120°C, the modulus increases with increasing temperature, probably because of oxidative crosslinking of the rubbery network. The rubbery plateau region is the narrowest for the epoxy with the highest T_g and crosslink

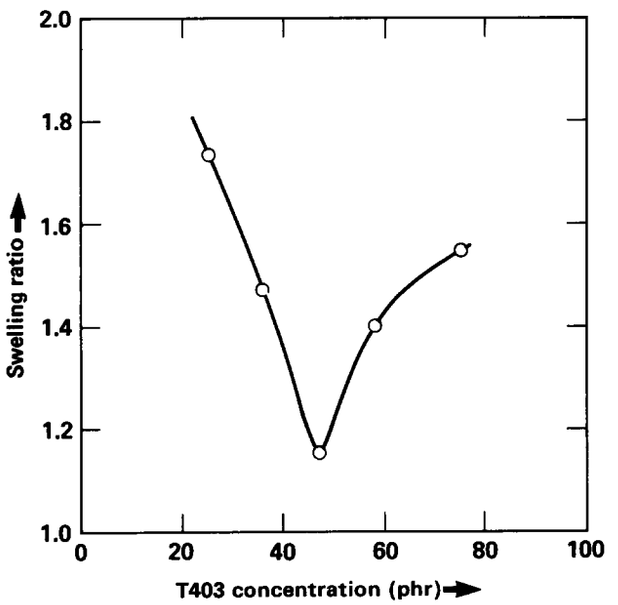

Figure 8 Swelling ratio *versus* T403 concentration for DGEBA–T403 epoxies, at 23°C

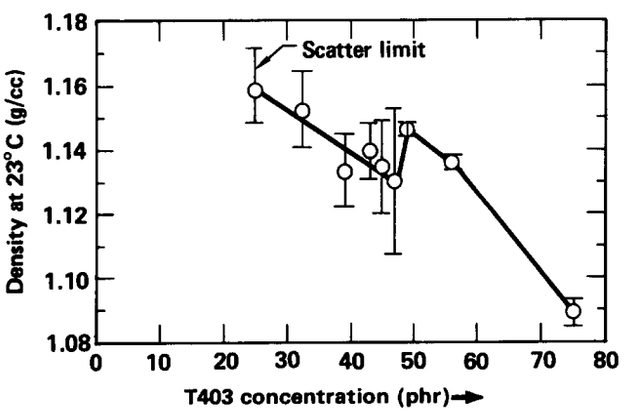

Figure 9 Density *versus* T403 concentration for DGEBA–T403 epoxies, at 23°C

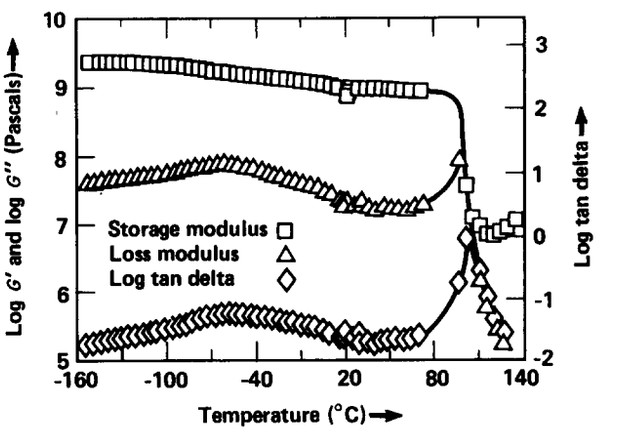

Figure 10 Dynamic mechanical properties of DGEBA–T403 (47 phr T403) epoxy

density, containing 47 phr T403, that is shown in *Figure 10*. For off-stoichiometric epoxies with lower T_g's and crosslink densities, the rubbery plateau is more distinct in the 100°–120°C range because the T_g is separated further from the onset of oxidative network degradation. M_c was determined from this data using Nielsen's[41] empirical equation:

$$\log_{10} G' \simeq 7.0 + 293d/M_c$$

where G' is the shear modulus in dynes cm^{-2} (10^{-1} Nm^{-2}) and d is the density of the polymer. The values of M_c determined from this equation as a function of T403 concentration are compared in *Figure 6* with the M_c–T403 concentration plot determined from the chemistry of the system as described previously. The experimental data points follow the same general trend as the chemically determined M_c–T403 concentration plot but exhibit on average ≈30% higher M_c values. The agreement between the data is relatively good in view of the empirical nature of the M_c–$\log_{10} G'$ relation and the inaccuracies in the M_c values determined from the chemical studies because of experimental errors in the values of the DGEBA and T403 equivalent weights and the concentration of unreacted epoxide groups.

Mechanical properties and deformation and failure processes

The DGEBA–T403 epoxies are ductile in tension at 23°C and exhibit a macroscopic yield point, and undergo necking and cold drawing.

The ultimate strain of the DGEBA–T403 epoxies exhibits a maximum of 15% at the stoichiometric T403 concentration as shown in *Figure 11*. (Chiao, Jessop, and Newey[5] also report a maximum in ultimate strain at the stoichiometric ratio for aromatic amine-cured DGEBA epoxies.) At ≲35 phr T403, the ultimate strain increases rapidly with decreasing T403 content as a result of increasing M_c, decreasing T_g, and plasticization of the glasses by unreacted DGEBA molecules. However, these ductile epoxy glasses which exhibit ≈70% strain to failure, embrittle over a period of days at 23°C (3% strain to failure) as a result of the recrystallization of the unreacted DGEBA molecules. A similar recrystallization phenomena in polyamide cured DGEBA epoxies has been reported previously[8].

In *Figure 12*, Young's modulus, E, for the DGEBA–T403 epoxies is plotted as a function of T403 concentration. At ≳35 phr T403, E decreases with increasing T403 concentration with a minimum super-imposed on this downtrend at the stoichiometric T403 concentration. A similar minimum is ioserved for the shear storage modulus G', determined from dynamic mechanical measurements, at the stoichiometric T403 concentration. Previously, a number of workers have observed a minimum in E in amine-cured epoxies at the stoichiometric curing agent concentration[3,5,6,9]. E rapidly decreases with decreasing T403 concentration of ≲35 phr T403 as a result of the increasing proximity of the T_g to the 23°C test temperature.

The tensile macroscopic yield stress and strength are plotted in *Figures 13* and *14*, respectively, as a function of T403 concentration. At ≳35 phr T403 both the macroscopic yield stress and tensile strength decrease with increasing T403 concentration. There is no evidence of a minimum superimposed on the downtrend in the yield stress and tensile strength at the T403 stoichiometric ratio. The yield stress and tensile strength for the T403 stoichiometric ratio epoxy occur at approximately greater than 6% strain, whereas the modulus, which does exhibit a minimum at the T403 stoichiometric ratio, is determined at 1% strain. Apparently, the mechanical properties measured at the higher strains are not sensitive to the geometric constraints imposed on the segmental

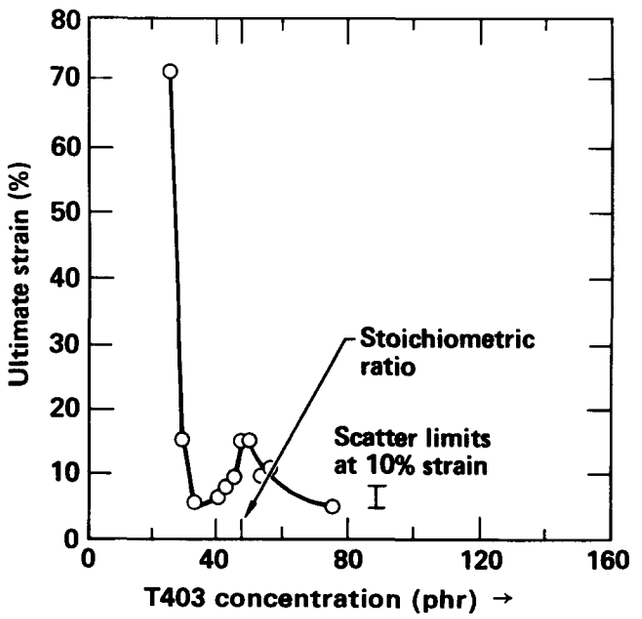

Figure 11 The ultimate tensile strain *versus* T403 concentration for DGEBA–T403 epoxies, at 23°C

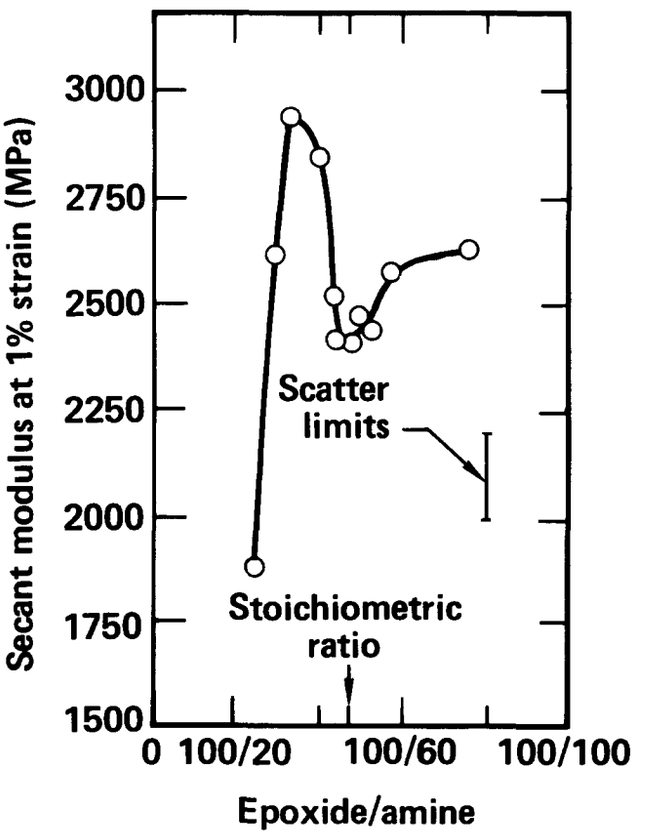

Figure 12 Tensile Young's modulus of DGEBA–T403 epoxies as a function of T403 concentration, at 23°C

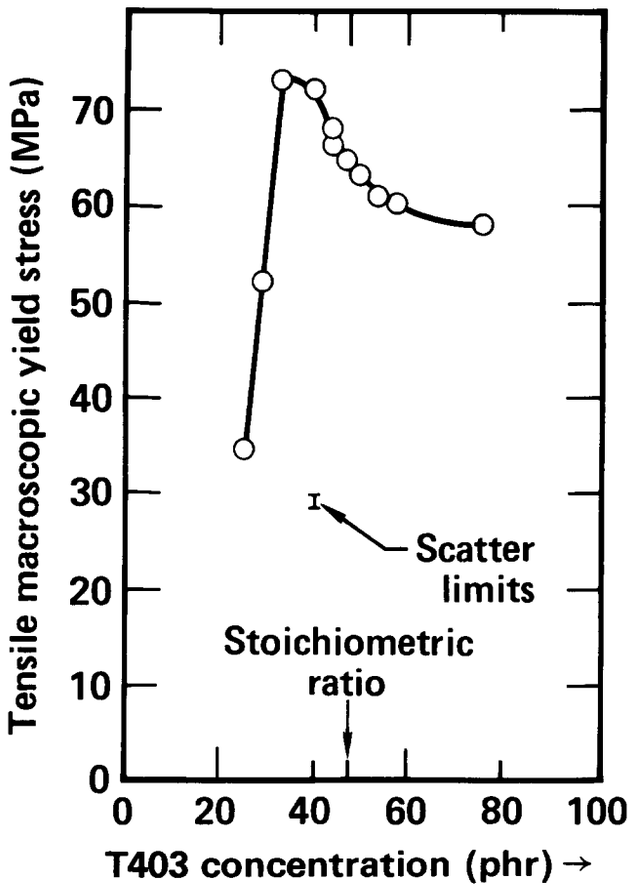

Figure 13 Tensile macroscopic yield stress of DGEBA–T403 epoxies as a function of T403 concentration, at 23°C

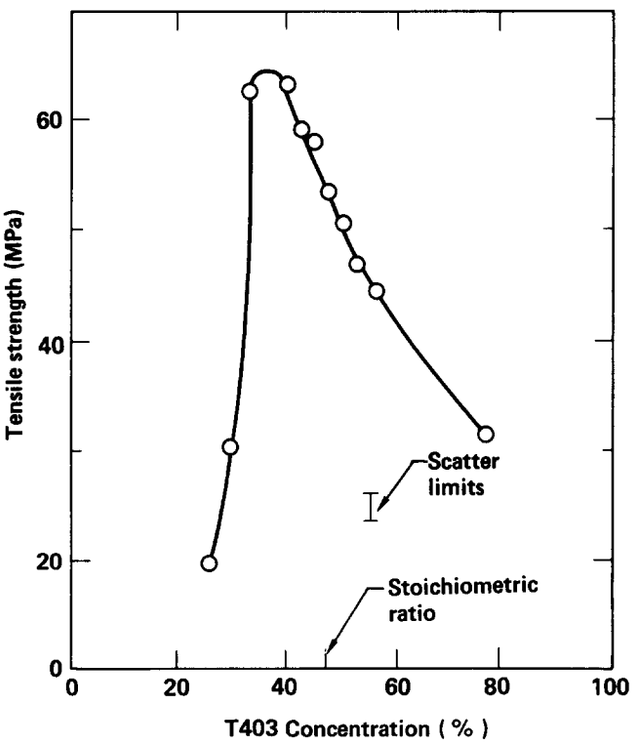

Figure 14 Tensile strength of DGEBA–T403 epoxies as a function of T403 concentration, at 23°C

packing by the network crosslinks. Mechanical property data of the DGEBA–T403 epoxy system reported by Chiao and Moore[4] in the 36–42 phr T403 range is consistent with the data shown in *Figures 13* and *14*. At <35% T403 concentration, the tensile yield stress and strength decrease rapidly with decreasing T403 concentration as a result of decreasing T_g, increasing M_c, and the plasticizing effect of unreacted DGEBA monomer. The microscopic yield stress, defined as that stress at the onset of the non-linear behaviour in the stress–strain plot, follows the same trend with T403 concentration as the macroscopic yield stress.

The mechanical properties of DGEBA–T403 epoxies are dependent on thermal history and the resultant glassy state free volume, as has been reported for other epoxy systems[12,27,42–45]. Annealing just below T_g decreases the glass-state free volume whereas quenching the epoxy from above its T_g results in a high free volume. A higher free volume enhances the ability of network segments to undergo flow under load via rotational isomeric configurational changes and results in a decrease in the yield stress and an increase in the ultimate elongation. For example, at 23°C for the DGEBA–T403 (47 phr T403) epoxy, there is a 70% increase in strain to failure and a 20% decrease in the yield stress for a glass that was quenched into ice water from 60°C above T_g relative to a glass that had been annealed for 24 h at 7°C below T_g. In addition, reversible thermal anneal cycles produced reversible changes in the mechanical properties of this epoxy because of the reversibility of the free volume changes.

The deformation processes of DGEBA–T403 epoxies were monitored under polarized light as a function of strain level. The birefringent patterns of DGEBA–T403 (47 phr T403) epoxy as a function of strain are shown in *Figure 15*. At strains ≤2.5% only elastic deformations occur and homogeneous colour changes produced under polarized light in this strain region disappear instantaneously upon removal of the load. In the 2.5–4% strain region, homogeneous elastic and plastic deformations occur, and upon removal of the load the homogeneous plastic deformation does not relax out which results in a permanent homogeneous colour change in the unstrained epoxy when viewed under polarized light. Above 4% strain, the plastic deformation becomes increasingly inhomogeneous with increasing strain as indicated by the development of birefringent fringes. Ultimately, a local region of high strain develops in the sample in the form of a diffuse shear band and a neck develops in this region. The birefringent fringes orient at ≈45° to the direction of the applied load in the shear band. Fracture occurs in the high strain, shear band region. Occasionally, more than one diffuse shear band will develop in the sample.

For the off-stoichiometric DGEBA–T403 epoxies that are in the 30–75 phr T403 range, birefringent-strain studies indicate the following trends in the deformation processes for epoxies that increasingly are removed further from the stoichiometric T403 concentration: (1) plastic flow is initiated and also becomes inhomogeneous at lower strains; (2) the regions of high strain are less oriented and their associated shear bands are less well developed upon crack propagation and ultimate failure through such regions. DGEBA–T403 epoxies in the 20–30 phr T403 range that exhibit ultimate elongations in the 20–70% range deform only in a homogeneous plastic fashion.

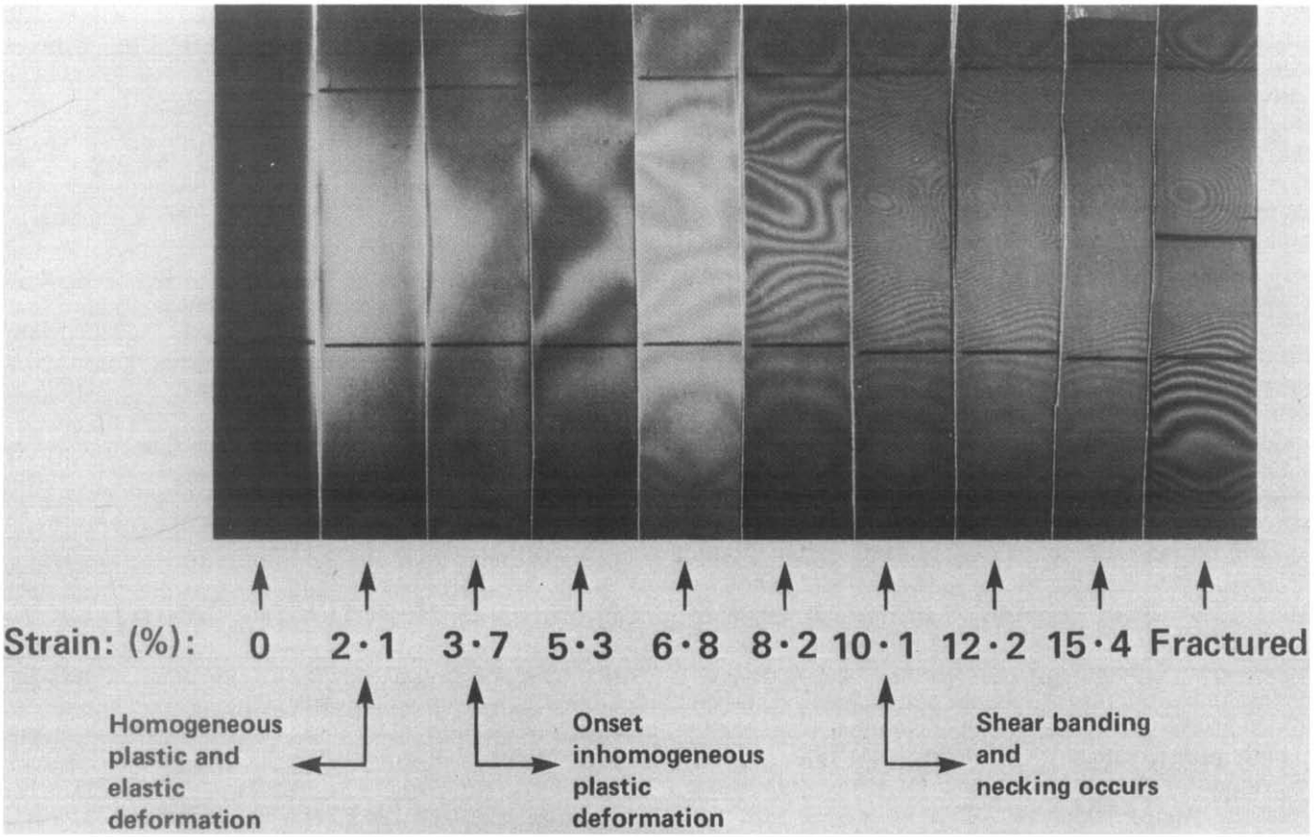

Figure 15 Birefringent deformation processes in DGEBA–T403 (47 phr T403) epoxy as a function of strain at 23°C, under polarized light

The fracture topographies of the DGEBA–T403 epoxies exhibit three characteristic regions: (1) a coarse initiation region; (2) a slow crack growth, smooth region; and (3) a fast crack growth, rough region. These topographical features are typical for tensile failures of unnotched amine-cured epoxies[8,13,27,29,30]. The coarse initiation region is a result of crack propagation through coarse crazes and/or shear bands. The crack then imposes a higher stress field on the craze or flaw tip which produces a small plastic zone that results in a smooth fracture topography. Whether flow in this small plastic zone at the crack tip occurs by shear yielding or yielding under normal stresses is difficult to ascertain experimentally and will depend on the stress fields imposed on the epoxy immediately ahead of the crack tip. The area of the mirror fracture topography is a measure of the ability of the polymeric glass to undergo plastic flow at the propagating crack tip. The percentage of the fracture surface that exhibits the smooth mirror topography for the DGEBA–T403 epoxies is plotted as a function of T403 concentration in *Figure 16*. This mirror area percentage exhibits a minimum near the stoichiometric T403 concentration, and nearly completely covers the fracture surface ± 25 phr T403 content on either side of stoichiometry. The least flow occurs ahead of the propagating crack for the stoichiometric epoxy because this glass is most highly strained prior to crack propagation.

Structural factors controlling mechanical properties and deformation and failure processes

The structural factors that control the deformation and failure processes and mechanical properties of DGEBA–T403 epoxies are here critically reviewed. It is suggested here that molecular failure processes and ultimate elongation of the DGEBA–T403 epoxies are controlled by the concentration of inherent and/or stress-induced defects in the most highly strained region of the epoxy network. In fully reacted networks, network failure is

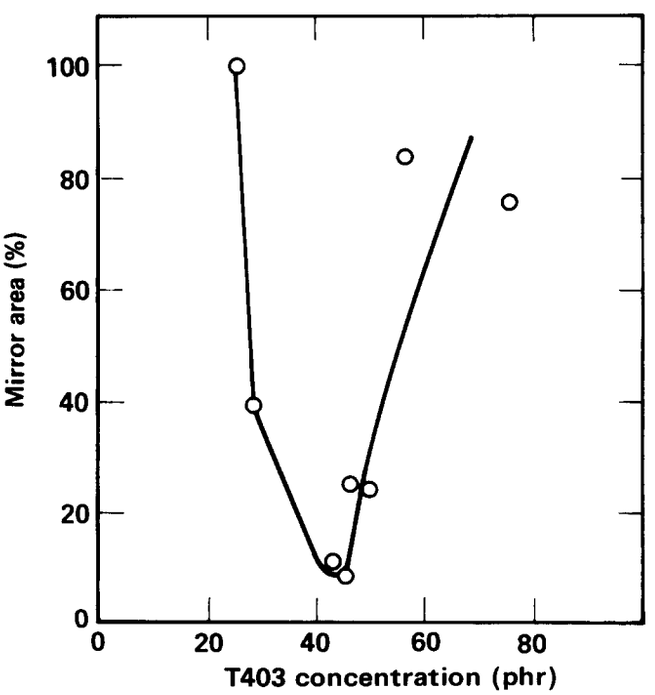

Figure 16 Mirror area as a percentage of total fraction surface *versus* T403 concentration for DGEBA–T403 epoxies fractured at 23°C

initiated by chain scission in overstrained segments. Such scissions result in the neighbouring segments carrying more of the applied load. Furthermore, the chemically active free radicals that form upon scission can react with neighbouring segments to produce further scissions. Both these phenomena result in autocatalytic network degradation. The scission process will depend directly on the network extensibility and, therefore, on the network topography. Evidence to support these contentions are now considered.

Consider first network deformation in the elastomeric state. A number of workers have developed expressions for the relation between the ultimate network mechanical properties and the crosslink density of an elastomeric network[46-49]. Such expressions assume the networks are randomly crosslinked and affine deformation occurs. For such networks, chain segments between crosslinks will experience tensions far larger or smaller than the average. Bueche[48] predicts at high crosslink densities that the strength of the rubbery networks rapidly decrease with decreasing M_c, because of the enhanced probability of fracture of chain segments. Experimental evidence supports Bueche's theory[46,48,50]. In the case of epoxies, however, the crosslinking process is not random because the molecular weight between the active chemical species in the unreacted epoxide and amine monomers generally exhibit discrete values. Primarily, there are three discrete M_c values for the fully crosslinked DGEBA–T403 epoxy network. An M_c value of 342 is associated with the DGEBA segment and M_c values of 100 and 158 are associated with the arms of the T403 molecule in which x, y or $z=1$ or 2, repsectively, in *Figure 1*. (Capillary column gas chromatography studies of T403 together with probability theory indicates that in $\approx 95\%$ of the T403 segment arms x, y, or $z=1$ or 2.) In *Figure 17*, the distribution in the M_c values of the fully cured DGEBA–T403 epoxy network is compared with a network that has the same average M_c between crosslinks, but exhibits a random distribution in M_c with arbitrarily assigned limits of M_c at 50–450. In randomly crosslinked networks under strain, computer modelling studies of such networks indicate the small percentage of the lowest M_c segments will carry a significant portion of the load and these segments will undergo chain scission at relatively low loads. For this randomly crosslinked network, a continual network degradation occurs under strain as a result of the progressive scission of the small percentage of unbroken,

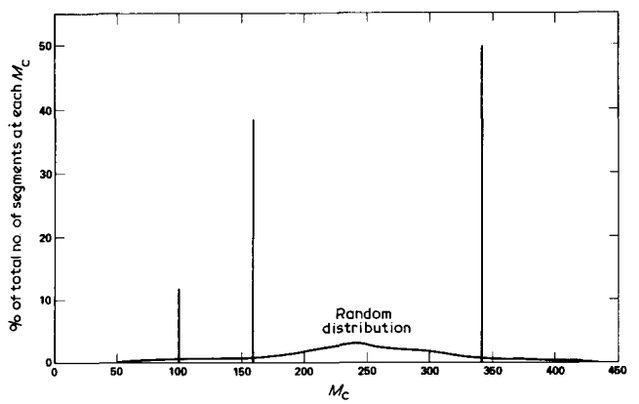

Figure 17 Distribution in the M_c values for fully-cured DGEBA–T403 (47% T403) epoxy compared with a random distribution of similar average M_c

lowest M_c segments that carry a significant portion of the applied load. In contrast, in the DGEBA–T403 network the percentage of segments with the lowest M_c value is $\approx 11.5\%$ of the total network segments and, hence, there are a considerably larger number of minimum M_c segments to share the load than in the case of the randomly crosslinked network. Nevertheless, the DGEBA–T403 network is far from ideal compared to most amine-cured DGEBA epoxies which contain segments of two discrete M_c values in which 50% of the segments exhibit the minimum M_c value.

The extensibility of the network segments rather than the M_c values determine the ultimate network properties. From the theory of rubber elasticity, the maximum network extensibility is directly related to M_c by the expression, $\lambda_b \propto M_c^{\frac{1}{2}}$[49]. In highly crosslinked systems, however, the extensibility of the network segments between crosslinks depends on specific rotational isomeric configurations of the segments and the perturbation of these configurations from their minimum energy configurations by geometric network constraints. In the case of the DGEBA–T403 network, molecular models indicate that the lowest M_c segments are indeed the least extensible. Hence, for the fully crosslinked DGEBA–T403 epoxy network in the elastomeric state the extensibility of the lowest M_c, least extensible segments and their concentration determine the ultimate network mechanical properties. The packing of the network in the elastomeric state determines the number of such segments in a specific plane and, hence, the load each minimum M_c segment carries under stress. In addition to the segmental extensibility, the network topography will also significantly affect the ultimate elastomeric network properties. Computer modelling indicates the abilities of the basic ring structures of the epoxy network (that are illustrated in *Table 2*) to undergo deformation control the network extensibility. Molecular modelling, together with computer modelling, indicates the deformability of these rings depends on (1) the extensibility of their sides; (2) the flexibility of their internal angles; and (3) their ability to undergo co-operative deformation with their interconnected neighbours. Their co-operative deformation is controlled by the regularity of the network topography which is determined by the different geometries of the basic rings and their orientation relative to one another. The more regular networks consist of interconnected rings of similar size and shape. However, the more irregular networks consist of rings with a variety of geometries that will develop overstrained segments at lower extensibilities. The fully crosslinked DGEBA–T403 epoxy network is relatively irregular as shown in *Table 1*. The deformability of the basic ring structures will also depend on the direction of the applied stress field relative to the ring structure. This orientation factor will significantly affect the networks that consist of regions of regularly oriented and interconnected rings.

In the glassy state, the flexibility and extensibility of the crosslinked epoxy network will be constrained by the available glassy-state free volume. This free volume will depend on the molecular shape and packing potential of the monomeric epoxide and amine constituents, the geometric constraints imposed on the packing of the network segments by the network topography and the proximity of the epoxy glass to its T_g. The ability of the chain segments to attain their maximum extended state via rotational isomeric changes will depend on the

intramolecular flexibility of the segments in addition to their intermolecular packing requirements[38]. The intensity of a glassy-state secondary T_{gg} is a crude indication of the glassy state flexibility of that portion of a network segment associated with the T_{gg}. In the case of the DGEBA–T403 epoxies the intensity of the principal glassy-state T_{gg} exhibits a maximum at stoichiometry, indicating the packing constraints imposed on the network segments by the crosslinks enhances local segmental mobility. Recent electron paramagnetic resonance studies of DGEBA–T403 epoxies by Brown and Sandreczki[51] also indicate mobility of free radicals in the glassy state is a maximum for the highest crosslink density epoxy.

In the DGEBA–T403 epoxy glasses there is sufficient segmental mobility in the highly-strained shear bands, through which ultimate fracture occurs, that the network structure and its associated defects rather than the glassy state packing constraints determine the ultimate strain in this region. Hence, the ultimate glassy-state extension in DGEBA–T403 epoxies is a maximum at stoichiometry and decreases either side of stoichiometry as more defects are introduced into the network in the form of unreacted groups. The presence of unreacted groups and their associated unconnected, non-load bearing segments results in higher loads being imposed under stress on those segments that are incorporated into the network. The higher segmental stresses enhance stress-induced chain scissions at lower network extensibilities. The critical concentration of chain scissions associated with crack initiation will be attained at increasingly lower network extensibilities as the initial concentration of unreacted groups in the network increases.

There is experimental evidence that network chain scission does occur during the deformation of DGEBA–T403 (47 phr T403) epoxies. Experiments have been carried out at LLNL[52] in which these epoxies have been strained homogeneously and plastically to 30% extension under tension at 70°C (ultimate failure is ≈40% at 70°C) and then the load removed and this strain completely annealed out at 100°C. Subsequent studies indicate the ductility of such epoxies decreased by 70% and their T_g's decrease by 8°C compared to reference specimens that were exposed to the same thermal history but were not stressed at 70°C. Such deterioration in the mechanical response and T_g are consistent with network deterioration via chain scission. In more direct evidence (1) stress-Fourier transform infra-red spectroscopy studies of thin DGEBA–T403 epoxy films indicate permanent chemical changes occur after removal of the load after 10% strain at 23°C[53] and (2) free radicals have been observed by electron paramagnetic resonance studies after ballmilling these epoxies.[51]

The magnitudes of the macroscopic and microscopic yield stresses, tensile strength (which is controlled by the flow properties of the epoxy) and Young's modulus, E, of DGEBA–T403 epoxies are determined by the glassy-state packing and free volume. These mechanical properties will follow the same trends as the density as a function of T403 concentration. The density of the DGEBA–T403 epoxies decreases with increasing T403 content with a slight minimum superimposed on such a downtrend at stoichiometry (*Figure 9*) because of the constraints of the crosslinks on the network packing efficiency. At ≳35 phr T403, the yield stresses, tensile strength, and Young's modulus all follow the same trend as the density and decrease with increasing T403 concentration. The minimum in the density at stoichiometry that is superimposed on the downtrend with increasing T403 concentration is revealed in the modulus data but is not clearly evident in the yield stress and tensile strength data. At ≲35 phr T403, the DGEBA–T403 epoxies become increasingly soft with decreasing T403 concentrations as a result of the increasing proximity of T_g to the test temperature lower M_c values and increasing concentrations of unreacted DGEBA monomer which acts as a plasticizer. This softening causes sharp decreases in the yield stresses, tensile strength and modulus with decreasing T403 content resulting in a maximum in such properties at ≈35 phr T403. The ultimate extension of these soft glasses is enhanced as a result of homogeneous plastic flow.

CONCLUSIONS

DGEBA–T403 epoxy glasses form exclusively from epoxide–amine addition reactions. Their T_g exhibits a maximum and their swell ratio a minimum at the highest crosslink density. These highly crosslinked glasses are ductile and undergo necking and plastic deformation. The plastic deformation initially occurs homogeneously, but ultimately develops inhomogeneously in the form of shear bands. Failure occurs in the high strain, shear band region. Computer models indicate the ultimate strain of these crosslinked glassy networks is determined by the concentration of unreacted and/or broken network segments. Stress-induced chain scission of network segments is determined by the concentration and extensibility of the least extensible segments. The ability of these epoxies to undergo plastic flow depends on: (1) the deformability of the basic network ring structures and their ability to undergo co-operative motion; and (2) the glassy-state free volume. The free volume depends on the molecular shape and packing ability of the constituent epoxide and amine portions of the network and the geometric constraints imposed on segmental packing by the network geometry.

ACKNOWLEDGEMENTS

The authors wish to acknowledge colleagues at LLNL, I. L. Chiu and D. M. Hoffmann for the dynamic mechanical measurements, J. Clarkson for the capillary column gas chromatography studies, E. T. Mones for assistance in sample preparation and mechanical testing, and J. K. Lepper and L. E. Nielsen for their stimulating discussions related to these studies.

REFERENCES

1 Lee, H. and Neville, K. 'Handbook of Epoxy Resins', McGraw-Hill, New York, 1967, chap. 6
2 Busso, C. J., Newey, H. A. and Holler, H. V. Proc. 25th Conf. of Reinforced Plastics/Composites Division of SPI, Washington, D.C., 1970
3 Chiao, T. T., Jessop, E. S. and Newey, H. A., 'A Moderate Temperature Curable Epoxy for Advanced Composites' Lawrence Livermore Laboratory Report UCRL-76126, 1974
4 Chiao, T. T. and Moore, R. L. Proc. 29th Conf. of Reinforced Plastics/Composites Division of SPI, Washington, D.C., Section 16-B, 1, 1974
5 Chiao, T. T., Jessop, E. S. and Newey, H. A. *SAMPE Quart.* 1974, **6**, 1
6 Selby, K. and Miller, L. E. *J. Mat. Sci.* 1975, **10**, 12
7 Pritchard, G. and Rhoades, G. V. *Mat. Sci. Eng.* 1976, **26**, 1
8 Morgan, R. J. and O'Neal, J. E. *J. Macromol. Sci. Phys.* 1978, **15**, 139

9 Kim, S. L., Skibo, M. D., Manson, J. A., Hertzberg, R. W. and Janiszewski, J. *Polym. Eng. Sci.* 1978, **18**, 1093
10 Phillips, D. C., Scott, J. M. and Jones, M. *J. Mat. Sci.* 1978, **13**, 311
11 Young, R. J. in 'Developments in Polymer Fracture—1,' (E. H. Andrews, Ed.) Appl. Sci. Publishers, London, 1979
12 Morgan, R. J. *J. Appl. Polym. Sci.* 1979, **23**, 2711
13 Morgan, R. J., O'Neal, J. E. and Miller, D. B. *J. Mat. Sci.* 1979, **14**, 109
14 Yamini, S. and Young, R. J. *J. Mat. Sci.* 1980, **15**, 1814
15 Scott, J. M., Wells, G. M., and Phillips, D. C., *J. Mat. Sci.* 1980, **15**, 1436
16 Lee, H. and Neville, K. 'Handbook of Epoxy Resins,' McGraw-Hill, New York, 1967, chap. 7
17 Kreahling, R. P. and Kline, D. E. *J. Appl. Polym. Sci.* 1969, **13**, 2411
18 Murayama, T. and Bell, J. P. *J. Polym. Sci. A-2* 1970, **8**, 437
19 French, D. M., Strecker, R. A. H. and Tompa, A. S. *J. Appl. Polym. Sci.* 1970, **14**, 599
20 Acitelli, M. A., Prime, P. B. and Sacher, E. *Polymer* 1971, **12**, 335
21 Prime, R. B. and Sacher, E. *Polymer* 1972, **13**, 455
22 Whiting, D. A. and Kline, D. E. *J. Appl. Polym. Sci.* 1974, **18**, 1043
23 Sidyakin, P. V. *Vysokomol. Soyed* 1972, **A14**, 979
24 Tanaka, Y. and Mika, T. F. in 'Epoxy Resins,' (C. A. May and Y. Tanaka, Eds.), Marcel Dekker, Inc., New York, 1973, Ch. 3
25 Bell, J. P. and McCavill, W. T. *J. Appl. Polym. Sci.* 1974, **18**, 2243
26 Dusek, K., Bleha, M. and Lunak, S. *J. Polym. Sci., Polym. Chem. Edn.* 1977, **15**, 2393
27 Morgan, R. J. and O'Neal, J. E. *Polym. Plast. Tech. Eng.* 1978, **10**, 49
28 Schneider, N. S., Sprouse, J. F., Hagnauer, G. L. and Gillham, J. K. *Polym. Eng. Sci.* 1979, **19**, 304
29 Morgan, R. J. and O'Neal, J. E. *J. Mat. Sci.* 1977, **12**, 1966
30 Morgan, R. J., Mones, E. T. and Steele, W. J. *Polymer* 1982, **23**, 295
31 Lee, H. and Neville, K. 'Handbook of Epoxy Resins,' McGraw-Hill, New York, 1967, chap. 5
32 Tanaka, Y. and Mika, T. F. in 'Epoxy Resins, Chemistry and Technology,' (C. A. May and Y. Tanaka, Eds.), Marcel Dekker, New York, 1973, chap. 3
33 Rinde, J. A. and Newey, H. A. *Composites Tech. Rev.* 1979, **1** (2) 4
34 Findley, W. N. and Reed, R. M. *Polym. Eng. Sci.* 1977, **27**, 837
35 Barton, J. M. *Polymer* 1979, **20**, 1018
36 Gordon, G. A. and Ravve, A. *Polym. Eng. Sci.* 1980, **20**, 70
37 Diamant, Y., Marom, G., and Broutman, L. J. *J. Appl. Polym. Sci.* 1981, **26**, 3015
38 Morgan, R. J. *J. Polym. Sci., Phys. Ed.* 1973, **11**, 1271
39 Morgan, R. J. and Nielson, L. E. *J. Macromol. Sci.-Phys.* 1974, **B9**(2), 239
40 Morgan, R. J. and O'Neal, J. E. *Polym. Plast. Tech. Eng.* 1975, **5**(2), 173
41 Nielsen, L. E. *J. Macromol. Sci.* 1969, **C3**, 69
42 Ophir, Z. N., Emerson, J. A., and Wilkes, G. L. *J. Appl. Phys.* 1978, **49**, 5032
43 Kaiser, J. *Makromol. Chem.* 1979, **180**, 573
44 Kong, E. S. W., Tant, M. R., Wilkes, G. L., Banthia, A. K. and McGrath, J. E. *Polym. Prepr.* 1979, **20**(2), 531
45 Kong, E. S. W., Wilkes, G. L., McGrath, J. E., Barthia, A. K., Mohajer, Y., and Tant, M. R. *Polym. Eng. Sci.* 1981, **21**, 943
46 Taylor, G. R. and Darin, S. R. *J. Polym. Sci.* 1955, **17**, 511
47 Beuche, A. M. *J. Polym. Sci.* 1956, **19**, 275
48 Bueche, F. *J. Polym. Sci.* 1957, **24**, 189
49 Kaelble, D. H., in 'Epoxy Resins, Chemistry and Technology', (C. A. May and Y. Tanaka, Eds.), Marcel Dekker, New York, 1973, chap. 5
50 Flory, P. J., Rabjohn, N. and Shaffer, M. C. *J. Polym. Sci.* 1949, **4**, 435
51 Brown, I. M. and Sandreczki, T. C., McDonnell Douglas Research Laboratories, St. Louis, personal communication
52 Kong, F. M. and Morgan, R. J., Lawrence Livermore National Laboratories, unpublished
53 Butler, N. and Morgan, R. J., Lawrence Livermore National Laboratories, unpublished